Supplementary Information:

PEGDA-based HistoBrick for increasing throughput of cryosectioning and immunohistochemistry in organoid and small tissue studies

Emilie Vuille-dit-Bille[*,&,1,2], Larissa Utz[&,3,4], Fiona E. Müllner[3,4], Valeria J. Arteaga-Moreta[3,4], Yanyan Hou[3,4], Stefan E. Spirig[3,4], Diane Ledroit-Paic[1], Sarah Heub[1], Jonas Goldowsky[1], Gilles Weder[†,1], Magdalena Renner[*,†,3,4]

[1]CSEM SA, Switzerland. [2]Institute of Mechanical Engineering, EPFL, Switzerland. [3]Institute of Molecular and Clinical Ophthalmology Basel, Switzerland. [4]Department of Ophthalmology, University of Basel, Switzerland.

[&]Authors contributed equally, [†] Authors share the senior authorship

[*]corresponding authors: emilie.vuille-dit-bille@csem.ch and magdalena.renner@iob.ch

FIJI macro for outer segments quantification:

(exemplary for one set of images, as mentioned in the methods, for each experiment color thresholds were set to clearly visualize the nuclei-containing and outer segment areas, respectively)

```
run("Fire");
run("Flatten");
run("16-bit");

run("Fire");
run("RGB Color");

// Color Thresholder 2.14.0/1.54f, Autogenerated macro, single images only!
min=newArray(3);
max=newArray(3);
filter=newArray(3);
a=getTitle();
run("HSB Stack");
run("Convert Stack to Images");
```

```
selectWindow("Hue");
rename("0");
selectWindow("Saturation");
rename("1");
selectWindow("Brightness");
rename("2");
min[0]=0;
max[0]=255;
filter[0]="pass";
min[1]=90;
max[1]=255;
filter[1]="pass";
min[2]=95;
max[2]=255;
filter[2]="pass";
for (i=0;i<3;i++){
  selectWindow(""+i);
  setThreshold(min[i], max[i]);
  run("Convert to Mask");
  if (filter[i]=="stop")  run("Invert");
}
imageCalculator("AND create", "0","1");
imageCalculator("AND create", "Result of 0","2");
for (i=0;i<3;i++){
  selectWindow(""+i);
  close();
}
selectWindow("Result of 0");
close();
selectWindow("Result of Result of 0");
rename(a);
// Colour Thresholding----------

run("Fill Holes");
```

```
//close both LUT images (fire) manually
run("Images to Stack", "use");
selectImage("Stack");
roiManager("Select", 0);
//use overlay brush tool and manually draw over selection
run("Flatten", "stack");
run("Stack to Images");
run("8-bit");
setOption("BlackBackground", false);
run("Convert to Mask");

//make selection
run("8-bit");
run("Convert to Mask");
run("Fill Holes");
run("Analyze Particles...", "size=1000.00-Infinity show=Masks");
run("Set Measurements...", "area mean perimeter display redirect=None decimal=3");
run("Analyze Particles...", "size=120000-Infinity include summarize add");
roiManager("Show All without labels");
roiManager("Measure");
```

Supplementary Figure legends:

Supplementary Figure 1: (**a**) Computer-Aided Design (CAD) design of the HistoBrick molds for 16-wells. (**b**) Dynamic viscosity at 37 °C (mean±SD). (**c**) Dynamic viscosity curves at 37 °C (n=3 for each embedding matrix, mean±SD).

Supplementary Figure 2: Additional cell type staining and examples of damaged outer segments caused by gelatine embedding. (**a-e**) Verification of various retinal cell types among all tested embedding materials and embedding conditions. Consecutive sections from the same blocks as shown in Figure 4 were stained. The stainings are Hoechst in grey for all and in green: (**a)** L-M OPSIN (red and green cones marker); (**b**) ONECUT2 (horizontal cell marker); (**c**), TRPM1 (ON bipolar cell marker); (**d**) RLBP1 (Müller cell marker); (**e**) Bassoon (ribbon synapse marker).

Bassoon, RLBP1 and TRPM1 are average Z projections, while L-M OPSIN and ONECUT2 are maximum Z projections (all scale bars: 50 µm). (**f**) PNA staining to visualize stained inner- and outer segments (scale bar: 10 µm). (**g-i**) Damaged outer segment examples cause by gelatine HistoBrick embedding: (**g**) Stretched outer segments, arrowhead; (**h**) Organoid with holes in outer segments and disrupted outer segments, arrowheads; (**i**) organoid with ripped off outer segments, arrowheads (all scale bars: 100 µm). All sections are 25 µm thick.

Supplementary Figure 3: Workflow for quantifying outer segment + inner segment areas in human retinal organoids. (**a**) Brightfield image of a human retinal organoid that was later embedded using OCT to show that OCT samples had outer segments (arrows) before embedding (scalebar: 100 µm). (**b**) Schematic illustration of the segmentation of a retinal organoid into PNA area and Hoechst area that subtracted from each other yield their OS+IS area. (**c**) Quantitative outer segment area workflow (scale bar: 100 µm), confocal images: PNA staining to mask the area containing OS+IS and Hoechst staining to mask the area containing nuclei. Color mapping and color threshold were used to create masks, segmentation of the masks generated continuous regions of interest (ROI) surrounding the entire organoids for Hoechst and PNA, respectively. The analysis was optimized to fill unstained central parts of the organoids to generate a continuous mask. The merged image of both channels with their segmentation is shown in Figure 4g. Non-retinal or unstructured regions of the organoids interfered with the quantification. Minimal adjustments were manually made when both channels did not have a similar, and continuous signal in these parts, in order to obtain a continuous mask in both channels (see red arrow heads): (**d**) Sometimes non-retinal regions needed to be manually included in both channels equally, or (**e**) non-retinal regions, like RPE, needed to be removed in both channels equally. Scale bars are 100 µm. (**f**) Scatter plot of the Hoechst area [mm^2] vs. OS+IS thickness ϑ [mm] for each individual sample. (**g**) Scatter plot of the Hoechst area [mm^2] vs. the OS+IS area [mm^2]. Violin plots showing (**h**) the median±quartiles of the area [mm^2] or (**i**) the diameter [mm] of human retinal organoids (n=16306 organoids from Spirig et al[1], re-analyzed for this study).

Supplementary Figure 4: Angle between cryoblock and knife during cryosectioning leads to tilting of sections. (**a**) Photograph of a HistoBrick cryoblock in the cryostat. (**b**) Adjacent sections of 100 µm thickness to visualize tilting. The sections are 20 µm thick. (scale bars: 5 mm). Wells and organoids appear successively on the sections from bottom right to top left. (**c**) Top view of a schematic retinal organoid (grey) with outer segments in magenta and an attached non-retinal part (blue) was illustrated in a simplified way to demonstrate some problems of analyzing

cryosections. Numbered lines indicate hypothetical sectioning planes at four different cutting angles. The corresponding numbered sections are displayed on the right. (**d**) Comparison of the conventional and the HistoBrick embedding method. Savings for several aspects in terms of time and reagents of HistoBrick vs. conventional embedding are calculated for different hypothetical experiments.

Supplementary Figure 5: Characterization of displaced cells outside the outer nuclear layer in aging organoids. (**a**) Immunohistochemistry staining of an exemplary organoid of week 52 for validation of the origin of the displaced nuclei outside of the ONL (scale bars: 100 µm, 10 µm for zoom-in images on the right). Arrowheads point to displaced nuclei in the region of outer segments. It is shown that the displaced nuclei are negative for SOX9 (Müller cell marker) and MiTF (Retinal pigment epithelium marker), while positive staining for both markers can be observed on the overview on the left. (**b-h**) Immunohistochemistry of retinal organoids of different ages using MAP2 (neuronal marker) and ARR3 (cone marker) of different sections of the same organoid for the indicated age. Consecutive sections (25 µm thick) from the same embedding experiment as in Figure 6 were used for this additional staining, thus the same batches as ages of organoids are valid (scale bar: 100 µm). Arrowheads point to displaced nuclei in the region of outer segments. (**i**) Scatter plot of the Hoechst area [mm^2] vs. OS+IS thickness ϑ [mm] for each individual organoid shown in Figure 6c-d. (**j**) Scatter plot of the Hoechst area [mm^2] vs. the OS+IS area [mm^2] for each individual organoid shown in Figure 6c-d.

References

1. Spirig, S. E. *et al.* Cell type-focused compound screen in human organoids reveals CK1 and MAPK11 inhibition protects cone photoreceptors from death. 2023.10.09.561525 Preprint at https://doi.org/10.1101/2023.10.09.561525 (2024).

Supplementary Figure 1

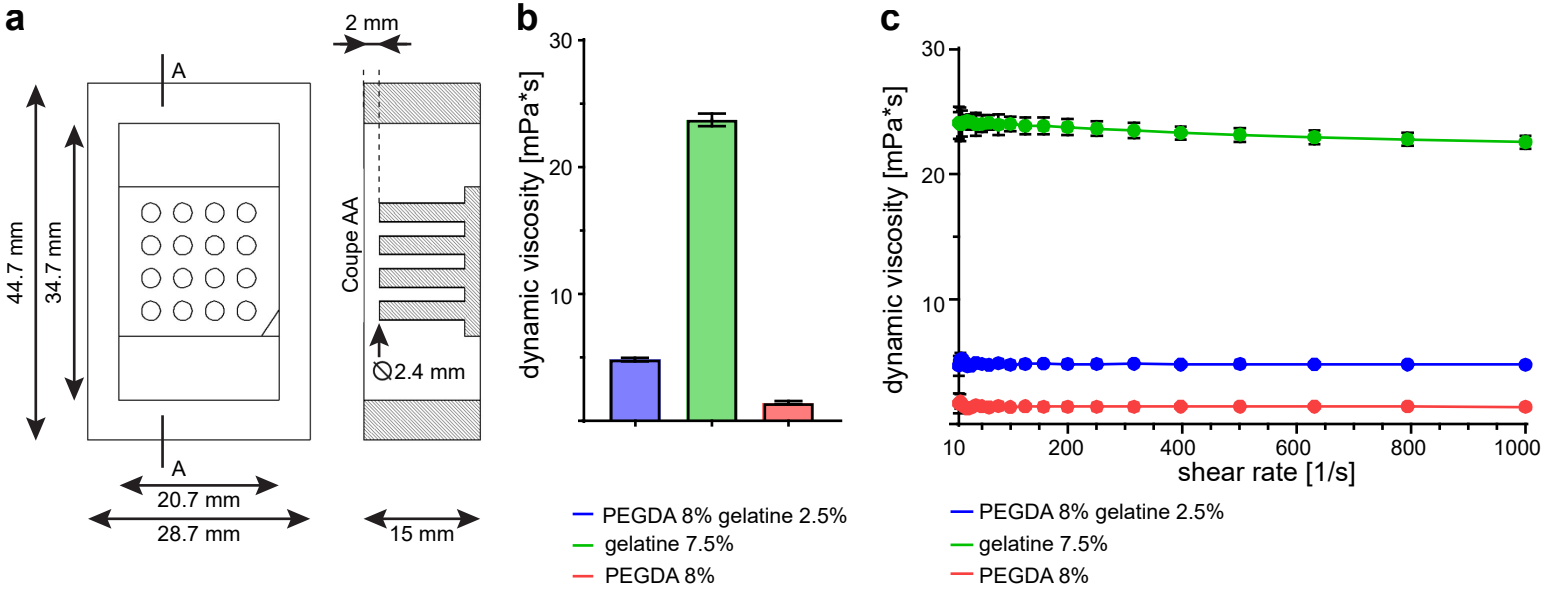

Supplementary Figure 2

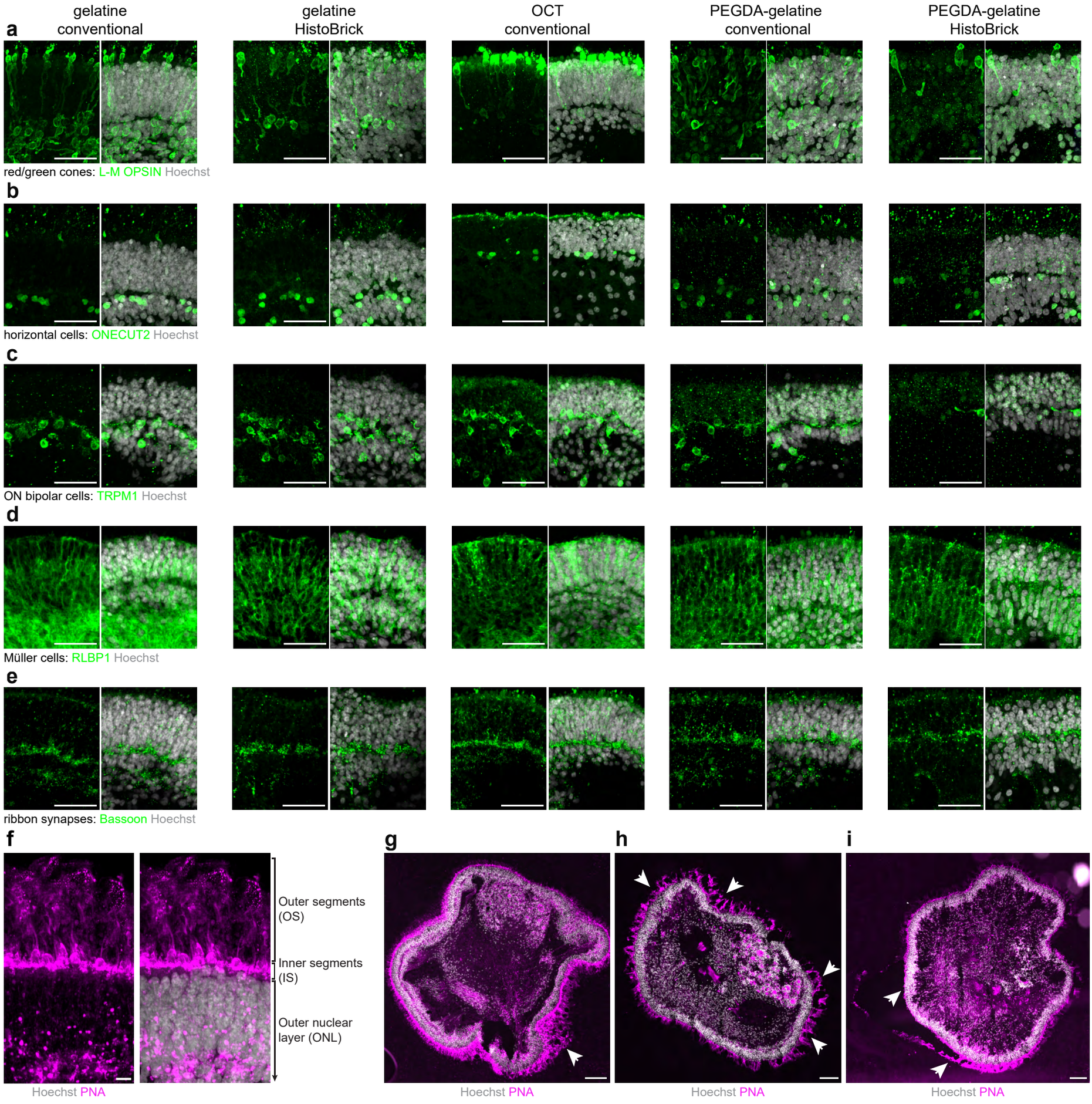

Supplementary Figure 3

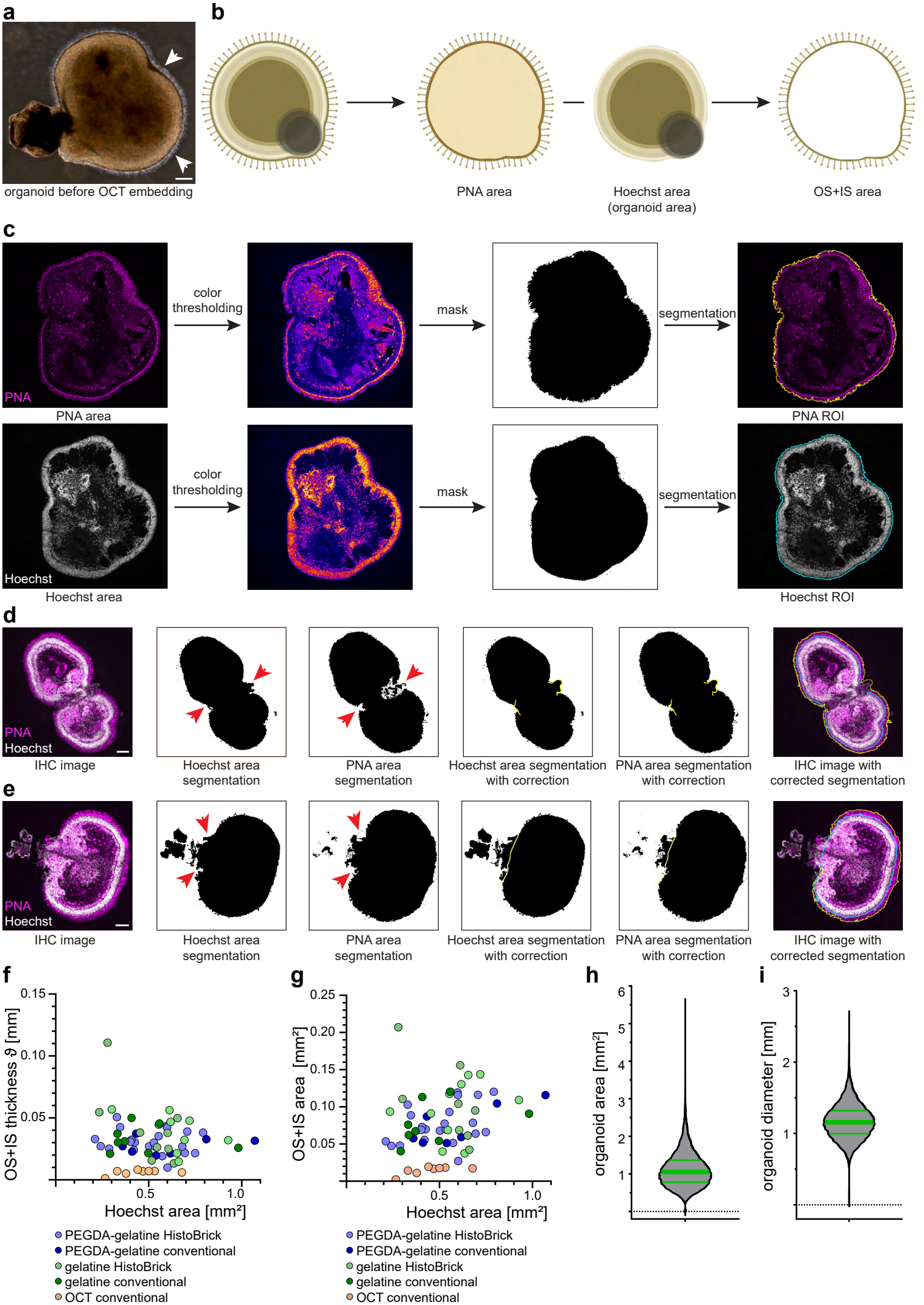

Supplementary Figure 4

a

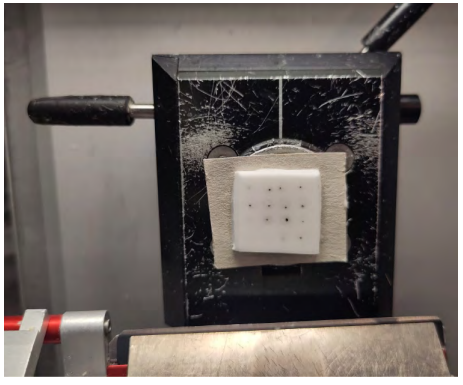

b

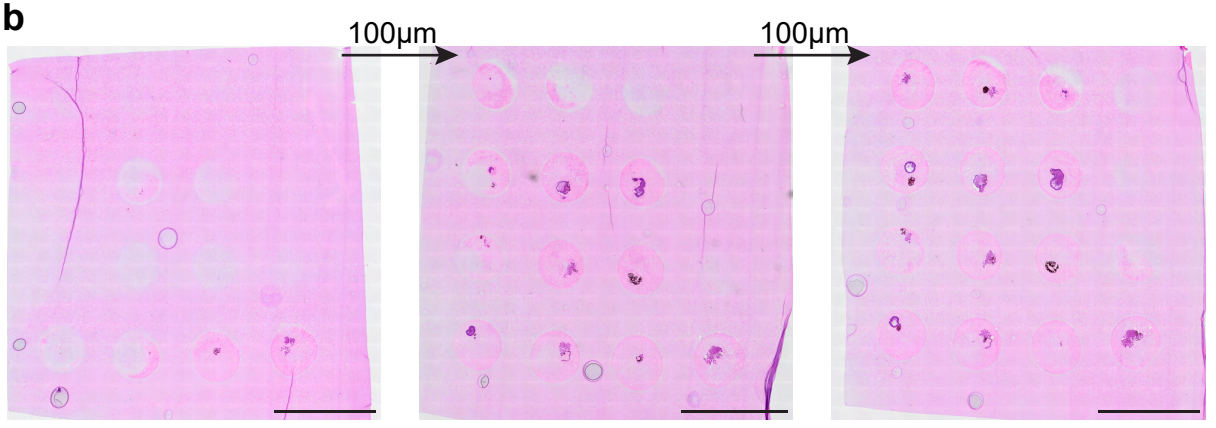

c

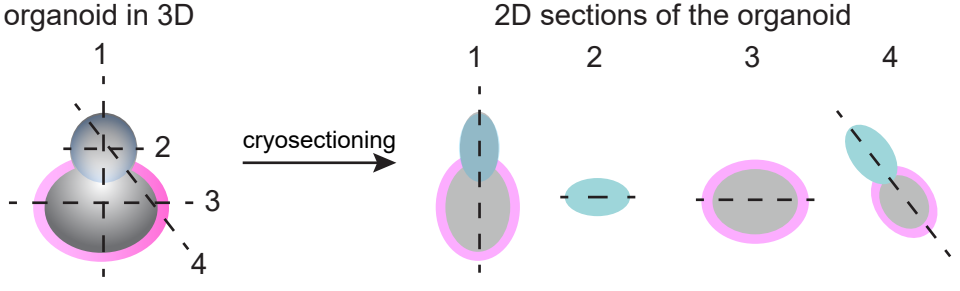

d

	reagents/time for 1 cryoblock		4 experimental conditions (n=4 organoids/experiment)			validation of 100 candidates from a screen, analyzing n=2 organoids per condition		
	conventional	HistoBrick	conventional	HistoBrick	HistoBrick savings compared to conventional [%]	conventional	HistoBrick	HistoBrick savings compared to conventional [%]
number of cryoblocks necessary	1	1	4	1	75	100	12.50	87.50
time to cut blocks (total h)	0.67	0.50	2.68	0.50	81.34	67	6.25	90.67
number of glass slides to collect sections	6	10	24	10	58.33	600	125	79.17
number of sections per slide	8	3	8	3		8	3	
reagents for 1st AB staining [µL]	180	180	720	180	75	18 000	2 250	87.50

Supplementary Figure 5